Mechanical Photoluminescence Excitation Spectra of a Strongly Driven Spin-Mechanical System

Xinzhu Li and Hailin Wang [*]

Department of Physics, University of Oregon, Eugene, Oregon 97403, USA

We report experimental studies of a driven spin-mechanical system, in which a nitrogen-vacancy (N-V) center couples to out-of-plane vibrations of a diamond cantilever through the excited-state deformation potential. Photoluminescence excitation studies show that in the unresolved sideband regime and under strong resonant mechanical driving, the excitation spectra of a N-V optical transition feature two spectrally sharp peaks, corresponding to the two turning points of the oscillating cantilever. In the limit that the strain-induced frequency separation between the two peaks far exceeds the N-V zero-phonon linewidth, the spectral position of the individual peak becomes sensitive to minute detuning between the mechanical resonance and the external driving force. For a fixed optical excitation frequency near the N-V transition, N-V fluorescence as a function of mechanical detuning features resonances with a linewidth that can be orders of magnitude smaller than the intrinsic linewidth of the mechanical mode. This enhanced sensitivity to mechanical detuning can potentially provide an effective mechanism for mechanical sensing, for example, mass sensing via measurements of induced changes in the mechanical oscillator frequency.

I. INTRODUCTION

In a driven spin-mechanical system, an electron spin or more generally an artificial atom, such as a defect center, couples to driven vibrations of a mechanical oscillator via direct or phonon-assisted transitions [1,2]. Driven spin-mechanical systems have been exploited for applications, such as the mechanical quantum control of electron or nuclear spins and the suppression of spin dephasing via dressed spin states [3–14]. For spin-mechanical systems that feature phonon-assisted (i.e., sideband) transitions, earlier experimental studies have emphasized the resolved-sideband regime, for which the mechanical frequency is large compared with the transition linewidth, since this regime is desirable for cooling and amplification of mechanical motion via spin-mechanical coupling [15,16], as well as for applications in quantum control, though experimental studies in the unresolved sideband regime have been carried out in nitrogen-vacancy (N-V) based as well as quantum-dot-based spin-mechanical systems [17–19].

In this paper, we report experimental studies of a driven spin-mechanical system in the unresolved sideband regime. For our system, a N-V center in a diamond cantilever couples to out-of-plane modes of the cantilever via the deformation potential of the N-V excited states and through the sideband optical transitions. Photoluminescence excitation (PLE) studies of the N-V center show

that under a strong external driving of the mechanical mode, the excitation spectra from a N-V optical transition feature two spectrally sharp peaks with a large strain-induced frequency separation, in contrast to the multiple sidebands observed in earlier experimental studies in the resolved sideband regime [20,21]. While the frequency separation increases linearly with the amplitude of the mechanical vibration, the linewidth of the peaks remains close to that of the zero-phonon line (ZPL). In the limit that the strain-induced frequency separation far exceeds the ZPL linewidth, N-V fluorescence at a given optical excitation frequency near the N-V transition becomes sensitive to minute detuning between the mechanical resonance and external driving force, even when the detuning is far smaller than the intrinsic linewidth of the mechanical mode. The resulting mechanical PLE spectra, i.e., N-V fluorescence as a function of mechanical detuning, feature resonances with a linewidth that can be orders of magnitude smaller than the intrinsic linewidth of the mechanical mode.

The greatly enhanced sensitivity to mechanical detuning can provide an effective mechanism for mechanical sensing [22], specifically, by monitoring frequency shifts of the mechanical oscillator through the sharp resonances in mechanical PLE. For earlier mechanical sensing studies, mechanical frequencies are monitored via piezoresistive, capacitive, optical interferometric, or optomechanical measurements. These measurements are limited by the intrinsic linewidth of the relevant mechanical mode.
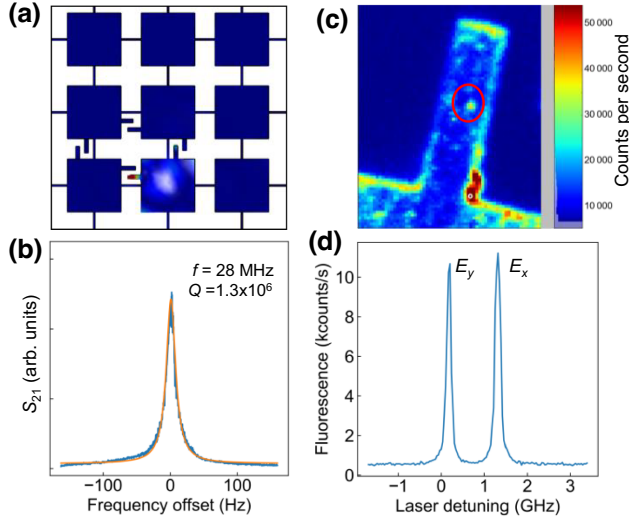
---

[*]hailin@uoregon.edu

FIG. 1. (a) Simulated displacement pattern of diamond cantilevers embedded in a square phononic crystal lattice with a period of 76 μm. The width and length of the bridge is 1.3 and 20 μm, respectively. (b) Spectral response of the fundamental out-of-plane mode of the cantilever used. (c) Confocal optical image of the cantilever. The red circle highlights the N-V center used in the PLE study. (d) PLE spectrum of the N-V center. The two ZPLs correspond to optical transitions from the $m_s = 0$ ground state to the E_x and E_y excited states.

II. EXPERIMENTAL METHOD

Diamond cantilevers used in this study feature a width of 4 μm, length near 15 μm, and a thickness near 2.5 μm. The cantilevers are embedded in a square phononic crystal lattice, as shown in Fig. 1(a). A phononic band gap of the square lattice protects the fundamental out-of-plane mode of the cantilevers from its surrounding environment [23]. The diamond phononic structure is fabricated from electronic grade single-crystal bulk diamond with {100} faces (from Element Six, Inc.), with electron-beam lithography and reactive ion etching. N-V centers are created about 100 nm below the diamond surface with ion implantation followed by stepwise high-temperature thermal annealing. Details of the sample fabrication are presented in earlier studies [24,25].

For the experimental results presented in this paper, the fundamental out-of-plane mode of the cantilever has a frequency, $\omega_m/2\pi = 28$ MHz, and a linewidth, $\gamma_m/2\pi = 22$ Hz, corresponding to a Q factor, $Q = 1.3 \times 10^6$ [see Fig. 1(b)]. The high Q factor results from the protection of the phononic band gap. The characterization of the mechanical modes is discussed in detail in our earlier study [23]. PLE studies are carried out in a N-V center near the middle of the cantilever, as shown in the confocal optical image in Fig. 1(c). The PLE spectrum of the N-V center obtained at $T = 8$ K and in the absence of external
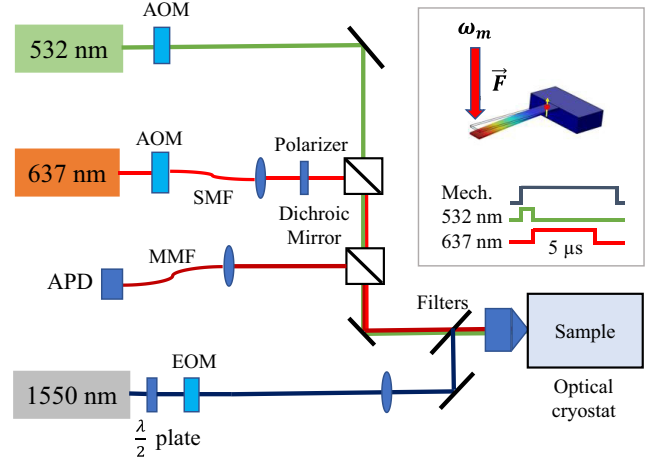

FIG. 2. Schematic of the experimental setup. AOM, acousto-optic modulator; APD, avalanche photodiode; MMF, multimode fiber; SMF, single mode fiber. The inset illustrates a schematic of resonantly driving the vibrations of the cantilever with radiation pressure force and shows the pulse sequence for the PLE experiment.

mechanical driving is characterized by two ZPLs, corresponding to the transitions from the $m_s = 0$ ground state to the E_x and E_y excited states [see Fig. 1(d)] [26]. The ZPLs feature a spectral linewidth near 100 MHz, indicating the high optical quality of the N-V center, though the spin-mechanical coupling via the sideband optical transitions is in the unresolved sideband regime.

Figure 2 shows a schematic of the experimental setup, which is based on a home-built low-temperature scanning confocal microscope. The thin diamond phononic structure is glued to a bulk diamond plate mounted on the cold finger of an optical cryostat (Montana Instrument S50). All experimental results presented in this paper are obtained with an estimated sample temperature of 8 K unless otherwise specified. For the PLE experiment, a green laser pulse ($\lambda = 532$ nm) initializes the N-V center into the $m_s = 0$ ground state. A tunable diode laser (New Focus Velocity TLB-6712) near 637.2 nm excites the N-V center. To avoid the power broadening of the ZPL, the red laser power is kept below 1 μW. N-V fluorescence with $\lambda > 645$ nm is collected with a $100\times$ objective (Nikon L Plan 0.85 NA) and then coupled into an optical fiber connecting to an avalanche photodiode (APD) for single-photon counting. The pulse sequence of the PLE experiment is shown in the inset of Fig. 2. Photon counting takes place when the 637.2-nm laser is on. An averaging time of 0.5 s is used for each data point in a PLE spectrum.

To resonantly drive the mechanical modes of the cantilever, we use radiation pressure force from a focused laser beam with $\lambda = 1.55$ μm, for which the intensity of the laser beam is sinusoidally modulated with an electro-optical modulator (EOM) and with a 100% modulation

depth. An additional lens is also used such that the 1.55-μm laser beam can be focused onto the cantilever surface along with the green and red laser beams. Pronounced mechanical spectral response [similar to that shown in Fig. 1(b)] can be observed with the driving laser power near 0.1 mW and with negligible contribution from thermal mechanical displacement, in agreement with theoretical expectations. Within the range of the laser power used (<50 mW), the mechanical displacement observed is proportional to the laser power. Note that optical powers given in the paper are measured before the 100× objective in the setup.

III. EXPERIMENTAL RESULTS AND ANALYSIS

A. Photoluminescence excitation of a driven spin-mechanical system

To investigate the coupling between the N-V center and the driven mechanical vibration, we measure the PLE spectra of the N-V center, while resonantly driving the fundamental out-of-plane mode. As shown in Fig. 3(a), at relatively weak mechanical driving, a broadening of the E_y resonance is observed, which is expected since the spin-mechanical system is in the unresolved band regime. With increasing mechanical driving and with other conditions remaining unchanged, two peaks appear in the PLE spectra of the E_y transition [see Fig. 3(b)]. Similar behaviors have also been observed in an earlier study [17]. The frequency separation between the two peaks is linearly proportional to the amplitude of the driving force, in this case, the average power of the 1.55-μm laser beam [see Fig. 3(c)]. Overall, the excitation spectra of the spin-mechanical system in the unresolved sideband regime differ qualitatively from those observed in the resolved sideband regime, which are characterized by distinct sideband resonances corresponding to emission or absorption of integer numbers of phonons [21].

To understand the excitation spectrum of the driven mechanical system in the unresolved sideband regime, we model the N-V center as a two-level system, which couples to the long wavelength mechanical vibration through the excited-state deformation potential, D. The electron-phonon interaction Hamiltonian describing the strain-induced energy shift of the excited state, $|e\rangle$, can be written as [20,27]

$$V_{e\text{-phonon}} = \hbar A \omega_m \sin(\omega_m t + \phi)|e\rangle \langle e|, \quad (1)$$

where A is a dimensionless driving amplitude proportional to both D and the amplitude of the mechanical vibration. For resonant or nearly resonant optical excitations, this interaction Hamiltonian leads to sideband optical transitions corresponding to the absorption or emission of integer numbers of phonons. To calculate the excited-state population of the N-V center, we solve the density-matrix

equations in the steady state, assuming that the N-V is initially in the $m_s = 0$ ground state and ω_m is large compared with the excited-state population decay rate. In the limit of weak optical excitation, the excited-state population for an optical excitation field with frequency ω is given by

$$\rho_{ee}(\omega) \propto \sum_{n=-\infty}^{+\infty} \frac{J_n^2(A)}{(\omega - \omega_0 - n\omega_m)^2 + (\gamma/2)^2}, \quad (2)$$

where γ and ω_0 are the linewidth and resonance frequency of the ZPL, respectively, and $J_n(x)$ is the Bessel function of the first kind. As shown in Eq. (2), the excitation of the N-V center includes the contributions from all relevant sidebands, i.e., phonon-assisted optical transitions, with a relative weighting determined by $J_n^2(A)$. Figures 3(d) and 3(e) show the theoretically calculated PLE spectra obtained for $A = 0, 1$ and for $A = 4, 12$, respectively, with $\gamma/2\pi = 100$ MHz. For $A \gg 1$, the frequency separation between the two PLE peaks derived from the calculation is linearly proportional to A. The small oscillations in Fig. 2(e) are remnants of phonon sidebands. For a direct comparison between the experimental and theoretical results, we plot in Fig. 3(c) the calculated frequency separation with a fixed conversion factor between A and the power of the 1.55-μm laser. A good agreement between the theory and experiment is achieved with 0.2-mW laser power corresponding to $A = 1$. The same conversion factor is also used for the theoretical results shown in Fig. 3(f).

The linear scaling between the frequency separation of the two peaks in the PLE spectra and the amplitude of the external driving force shown in Fig. 3(c) suggests a classical interpretation of the PLE spectra at relatively large A. In this case, the frequency separation corresponds to the strain-induced relative shift of the excited state between the two turning points, i.e., the maximum displacements of the cantilever vibration. Furthermore, the excitation spectra at the turning points are expected to retain the spectrally sharp N-V zero-phonon resonance except for a spectral shift. This is confirmed by the experimental and theoretical results shown, respectively, in Figs. 3(b) and 3(e). The experimental results on the linewidth of the PLE peaks as a function of the 1.55-μm laser power shown in Fig. 3(f) provide additional confirmation. As shown in Fig. 3(f), after a large increase in the linewidth, which occurs before the two peaks appear, the linewidth at relatively large A returns to values, which only slightly exceed the ZPL linewidth. The measured linewidths are also in general agreement with the calculated linewidths plotted in Fig. 3(f). For the asymmetric PLE peaks, we use a Lorentzian fit from the steep side of the peak to extract the linewidth [see Figs. 3(b) and 3(e)]. The variations in the linewidths under strong mechanical driving shown in Fig. 3(f) are to a large extent due to the variations in the curve fitting.

It should be noted that results similar to those shown in Fig. 3 are also observed for the E_x transition, for which
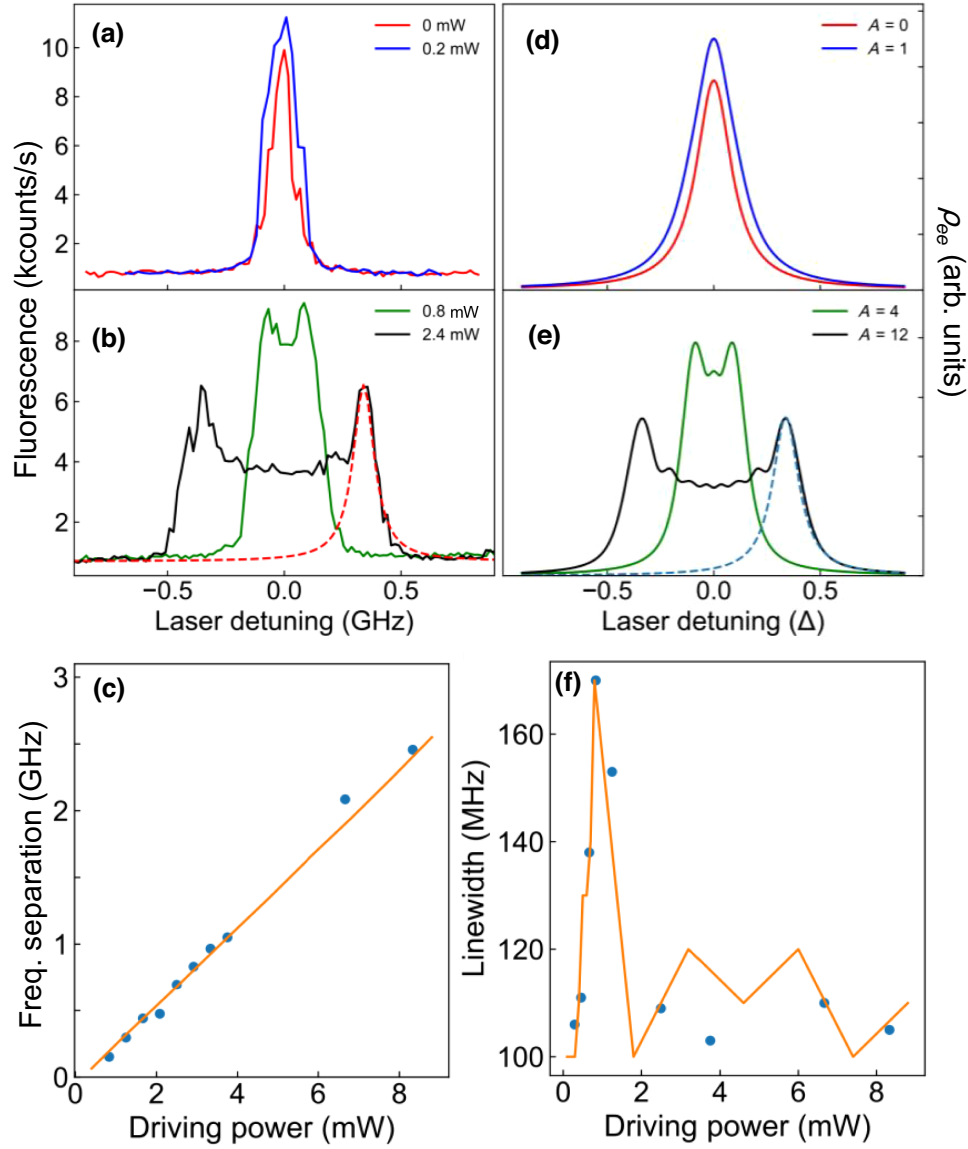
FIG. 3.   (a),(b) PLE spectra of the N-V center under resonant mechanical driving, with the 1.55-μm laser average power indicated in the figure. (c) Frequency separations of the two peaks in PLE spectra as a function of the mechanical driving power. (d),(e) Theoretically calculated PLE spectra as discussed in the text. The dashed line is a Lorentzian fit to the steep side of the peak. (f) Spectral linewidth of the PLE peaks versus the mechanical driving power. The solid lines in (c),(f) are derived from the theoretically calculated PLE spectra, for which a conversion factor of 0.2-mW laser power corresponding to $A = 1$ is used.

the strain-induced frequency separation between the two peaks in PLE spectra is about 50% of that observed for the E_y transition. In the limit that the frequency separation far exceeds the ZPL linewidth, nearly the same linewidth of the PLE peaks have been observed for both transitions.

B. Mechanical photoluminescence excitation

In the limit that the strain-induced frequency separation between the two PLE peaks far exceeds the ZPL linewidth, the PLE spectra depends sensitively on mechanical detuning (i.e., the detuning between the modulation frequency

of the 1.55-μm laser and the resonance frequency of the mechanical mode), even when the detuning is small compared with γ_m, as shown in Figs. 4(a) and 4(b). Figures 4(c) and 4(d) plot the N-V fluorescence obtained as a function of the mechanical detuning at two different 1.55-μm laser powers, where the optical excitation frequency is fixed near a peak of the corresponding PLE spectrum obtained at zero mechanical detuning.

The N-V fluorescence versus mechanical detuning shown in Figs. 4(c) and 4(d) can be viewed as mechanical PLE (MPLE), for which varying the mechanical detuning effectively shifts the resonance frequency of the N-V
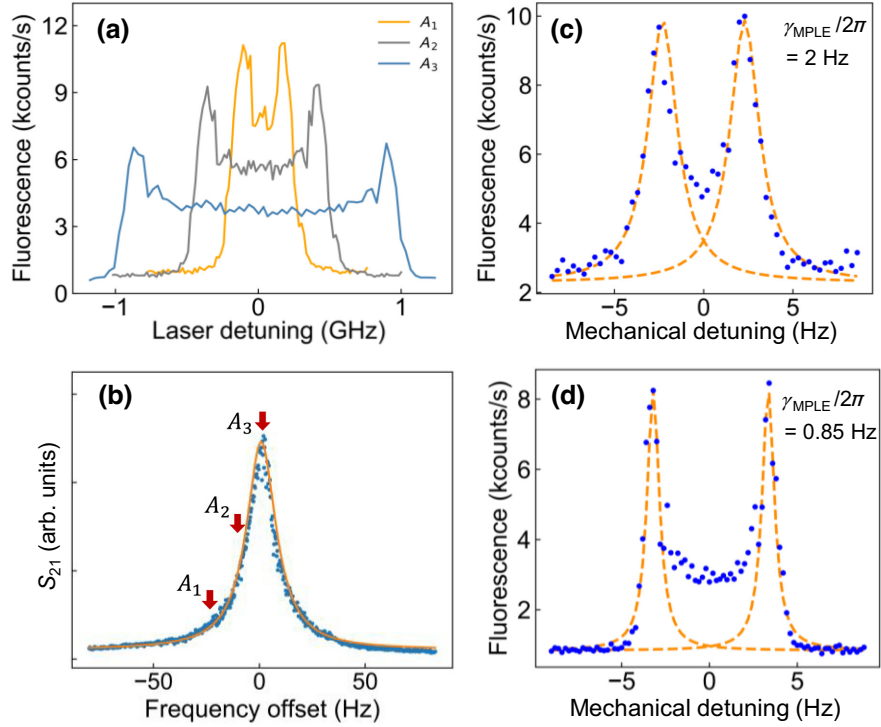
FIG. 4. (a) PLE spectra of the N-V center obtained with a 1.55-μm laser power of 6 mW, with the mechanical detuning indicated in (b). (b) Mechanical frequencies (indicated by the arrows) used for the PLE spectra in (a) relative to the resonance of the fundamental out-of-plane mode of the cantilever. (c) N-V fluorescence as a function of the frequency detuning of the mechanical drive, obtained with a 1.55-μm laser power of 9 mW and with the optical excitation frequency fixed near a peak of the corresponding PLE spectrum obtained at zero mechanical detuning. The dashed lines are Lorentzian fits to the steep side of the resonances. (d) The same as (c) except for a 1.55-μm laser power of 14 mW.

optical transition. These spectra are characterized by two sharp resonances. Each resonance occurs at a mechanical detuning, for which the spectrally shifted optical transition at a turning point of the mechanical oscillation is resonant with the optical excitation field. The MPLE spectra shown in Figs. 4(c) and 4(d) feature the unusual behavior that the linewidth of the individual resonance, γ_{MPLE}, can be orders of magnitude smaller than the intrinsic mechanical linewidth, γ_m. Furthermore, the stronger the external mechanical drive, the sharper the resonance becomes.

As shown in Fig. 4(a), the spectral position, s, of the N-V optical transition at a cantilever turning point shifts with mechanical tuning, δ. For a MPLE resonance centered at δ_0, the linewidth of the resonance is determined by the mechanical detuning needed to induce a frequency shift of γ for the corresponding N-V transition, i.e.,

$$\gamma_{\mathrm{MPLE}} \times \left.\frac{ds}{d\delta}\right|_{\delta=\delta_0} \approx \pm\gamma. \tag{3}$$

In the limit that $S/\gamma \gg 1$, where S is the strain-induced frequency separation between the two peaks in the PLE

spectra obtained at $\delta = 0$, we have

$$\gamma_{\mathrm{MPLE}} \approx \frac{(4\delta_0^2 + \gamma_m^2)^2}{4|\delta_0|\gamma_m^2} \times \frac{\gamma}{S}. \tag{4}$$

For Figs. 4(c) and 4(d), $|\delta_0|/2\pi = 2.3$ and 3.5 Hz and $S/2\pi = 2.97$ and 4.62 GHz [derived from the linear dependence between S and the 1.55-μm laser power in Fig. 3(c)], respectively. Theoretical estimates using Eq. (4) yield $\gamma_{\mathrm{MPLE}}/\gamma_m = 0.088$ and 0.041, in agreement with the experimentally obtained linewidth reduction, $\gamma_{\mathrm{MPLE}}/\gamma_m = 0.091$ and 0.039, for Figs. 4(c) and 4(d), respectively.

The sharp resonance in an MPLE spectrum can provide an effective mechanism to enhance the sensitivity of mechanical oscillator-based sensing [22], for example, mass sensing by monitoring the frequency shift of the mechanical oscillator [28–30]. The diamond cantilever used in this study has a mass near 0.5 nanogram. A mass change of 1 attogram results in a frequency shift of order 0.03 Hz. As shown in Fig. 4(d), the linewidth of the resonances in the MPLE is 0.85 Hz, compared with the intrinsic mechanical linewidth of 22 Hz. A greater reduction in the linewidth can be achieved with a stronger external mechanical drive. For the experimental implementation of
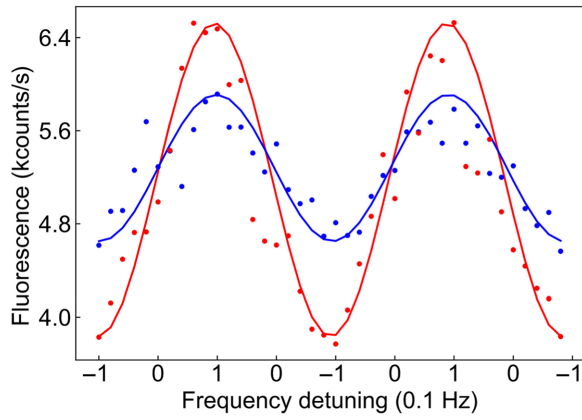
FIG. 5. N-*V* fluorescence as a function of oscillating mechanical detuning. The solid lines are least-squares fits to sinusoidal oscillations. For red (and blue) dots, a 1.55-μm laser power of 11 (and 6) mW is used, with other conditions nearly the same as those for Fig. 4.

mechanical sensing, a straightforward approach is to monitor the N-*V* fluorescence while fixing the frequency of the nearly resonant external mechanical drive near the middle of the steep slope of a resonance in the MPLE spectrum.

To determine the sensitivity for measuring mechanical frequency shifts, we monitor the N-*V* fluorescence while sinusoidally varying the mechanical detuning (see Fig. 5), where the zero frequency-detuning corresponds to the midpoint of the steep side of an MPLE resonance. The sensitivity for the frequency-shift measurement can be defined as [31]

$$\eta = \frac{\sigma^{1s}}{|dF/d\delta|}, \tag{5}$$

where σ^{1s} is the uncertainly for the fringe contrast F for 1 s averaging and $dF/d\delta$ is the gradient of F with respect to the mechanical detuning. From the results shown in Fig. 5, we estimate that $\eta = 0.01$ and 0.02 Hz/$\sqrt{\text{Hz}}$ when a 1.55-μm laser power of 11 and 6 mW is used, respectively. The better sensitivity at stronger mechanical driving arises from the increase in the gradient due to the reduction in γ_{MPLE}. For comparison, frequency noise floor for traditional mass-sensing experiments using cantilevers with $Q < 5000$ typically exceeds 0.1 Hz/$\sqrt{\text{Hz}}$ [28,29]. Note that the sensitivity shown in Fig. 5 is limited by the relatively small photon count rate used in the experiment and can thus be significantly improved.

IV. CONCLUSION

In summary, using a diamond cantilever as a model spin-mechanical system, we show that in the unresolved sideband regime and under strong resonant mechanical driving, the excitation spectra of a N-*V* optical transition feature two sharp peaks, corresponding to the two turning points of the oscillating cantilever. In the limit that the strain-induced frequency separation between the two peaks is large compared with the ZPL linewidth, the spectral position of the individual peak becomes highly sensitive to minute detuning of the mechanical drive, leading to sharp resonances in mechanical PLE spectra with a linewidth, which can be orders of magnitude smaller than the intrinsic mechanical linewidth. This enhanced sensitivity to mechanical detuning can provide an effective mechanism for mechanical sensing, for example, mass sensing via measurements of induced mechanical frequency shifts. While an N-*V* center has been used in this study, similar spin-mechanical processes and their potential applications can also be pursued in other defect or material systems.

[1] D. Lee, K. W. Lee, J. V. Cady, P. Ovartchaiyapong, and A. C. B. Jayich, Topical review: Spins and mechanics in diamond, J Opt. UK **19**, 033001 (2017).

[2] H. L. Wang and I. Lekavicius, Coupling spins to nanomechanical resonators: Toward quantum spin-mechanics, Appl. Phys. Lett. **117**, 230501 (2020).

[3] S. K. Hong, M. S. Grinolds, P. Maletinsky, R. L. Walsworth, M. D. Lukin, and A. Yacoby, Coherent mechanical control of a single electronic spin, Nano Lett. **12**, 3920 (2012).

[4] E. R. MacQuarrie, T. A. Gosavi, N. R. Jungwirth, S. A. Bhave, and G. D. Fuchs, Mechanical Spin Control of Nitrogen-Vacancy Centers in Diamond, Phys. Rev. Lett. **111**, 227602 (2013).

[5] J. Teissier, A. Barfuss, P. Appel, E. Neu, and P. Maletinsky, Strain Coupling of a Nitrogen-Vacancy Center Spin to a Diamond Mechanical Oscillator, Phys. Rev. Lett. **113**, 020503 (2014).

[6] E. R. MacQuarrie, T. A. Gosavi, A. M. Moehle, N. R. Jungwirth, S. A. Bhave, and G. D. Fuchs, Coherent control of a nitrogen-vacancy center spin ensemble with a diamond mechanical resonator, Optica **2**, 233 (2015).

[7] E. R. MacQuarrie, T. A. Gosavi, S. A. Bhave, and G. D. Fuchs, Continuous dynamical decoupling of a single diamond nitrogen-vacancy center spin with a mechanical resonator, Phys. Rev. B **92**, 224419 (2015).

[8] A. Barfuss, J. Teissier, E. Neu, A. Nunnenkamp, and P. Maletinsky, Strong mechanical driving of a single electron spin, Nat. Phys. **11**, 820 (2015).

[9] D. A. Golter, T. Oo, M. Amezcua, I. Lekavicius, K. A. Stewart, and H. Wang, Coupling a Surface Acoustic Wave to an Electron Spin in Diamond via a Dark State, Phys. Rev. X **6**, 041060 (2016).

[10] D. A. Golter, T. Oo, M. Amezcua, K. A. Stewart, and H. Wang, Optomechanical Quantum Control of a Nitrogen-Vacancy Center in Diamond, Phys. Rev. Lett. **116,** 143602 (2016).

[11] S. J. Whiteley, G. Wolfowicz, C. P. Anderson, A. Bourassa, H. Ma, M. Ye, G. Koolstra, K. J. Satzinger, M. V. Holt, F. J. Heremans, A. N. Cleland, D. I. Schuster, G. Galli, and D. D. Awschalom, Spin-phonon interactions in silicon carbide addressed by Gaussian acoustics, Nat. Phys. **15,** 490 (2019).

[12] S. Maity, L. Shao, S. Bogdanović, S. Meesala, Y.-I. Sohn, N. Sinclair, B. Pingault, M. Chalupnik, C. Chia, L. Zheng, K. Lai, and M. Lončar, Coherent acoustic control of a single silicon vacancy spin in diamond, Nat. Commun. **11,** 193 (2020).

[13] S. Maity, B. Pingault, G. Joe, M. Chalupnik, D. Assumpção, E. Cornell, L. Shao, and M. Lončar, Mechanical Control of a Single Nuclear Spin, Phys. Rev. X **12,** 011056 (2022).

[14] O. Arcizet, V. Jacques, A. Siria, P. Poncharal, P. Vincent, and S. Seidelin, A single nitrogen-vacancy defect coupled to a nanomechanical oscillator, Nat. Phys. **7,** 879 (2011).

[15] I. Wilson-Rae, P. Zoller, and A. Imamoglu, Laser Cooling of a Nanomechanical Resonator Mode to its Quantum Ground State, Phys. Rev. Lett. **92,** 075507 (2004).

[16] K. V. Kepesidis, S. D. Bennett, S. Portolan, M. D. Lukin, and P. Rabl, Phonon cooling and lasing with nitrogen-vacancy centers in diamond, Phys. Rev. B **88,** 064105 (2013).

[17] K. W. Lee, D. Lee, P. Ovartchaiyapong, J. Minguzzi, J. R. Maze, and A. C. B. Jayich, Strain Coupling of a Mechanical Resonator to a Single Quantum Emitter in Diamond, Phys. Rev. Appl. **6,** 034005 (2016).

[18] I. Yeo, P. L. de Assis, A. Gloppe, E. Dupont-Ferrier, P. Verlot, N. S. Malik, E. Dupuy, J. Claudon, J. M. Gerard, A. Auffeves, G. Nogues, S. Seidelin, J. P. Poizat, O. Arcizet, and M. Richard, Strain-mediated coupling in a quantum dot-mechanical oscillator hybrid system, Nat. Nanotechnol. **9,** 106 (2014).

[19] J. Kettler, N. Vaish, L. M. de Lepinay, B. Besga, P. L. de Assis, O. Bourgeois, A. Auffeves, M. Richard, J. Claudon, J. M. Gerard, B. Pigeau, O. Arcizet, P. Verlot, and J. P. Poizat, Inducing micromechanical motion by optical excitation of a single quantum dot, Nat. Nanotechnol. **16,** 283 (2021).

[20] M. Metcalfe, S. M. Carr, A. Muller, G. S. Solomon, and J. Lawall, Resolved Sideband Emission of InAs/GaAs Quantum Dots Strained by Surface Acoustic Waves, Phys. Rev. Lett. **105,** 037401 (2010).

[21] H. Y. Chen, E. R. MacQuarrie, and G. D. Fuchs, Orbital State Manipulation of a Diamond Nitrogen-Vacancy Center Using a Mechanical Resonator, Phys. Rev. Lett. **120,** 167401 (2018).

[22] A. Boisen, S. Dohn, S. S. Keller, S. Schmid, and M. Tenje, Cantilever-like micromechanical sensors, Rep. Prog. Phys. **74,** 036101 (2011).

[23] X. Li, I. Lekavicius, and H. Wang, Diamond nanomechanical resonators protected by a phononic band gap, Nano Lett. **22,** 10163 (2022).

[24] I. Lekavicius, T. Oo, and H. L. Wang, Diamond Lamb wave spin-mechanical resonators with optically coherent nitrogen vacancy centers, J. Appl. Phys. **126,** 214301 (2019).

[25] I. Lekavicius and H. L. Wang, Optical coherence of implanted silicon vacancy centers in thin diamond membranes, Opt. Express **27,** 31299 (2019).

[26] G. D. Fuchs, V. V. Dobrovitski, R. Hanson, A. Batra, C. D. Weis, T. Schenkel, and D. D. Awschalom, Excited-State Spectroscopy using Single Spin Manipulation in Diamond, Phys. Rev. Lett. **101,** 117601 (2008).

[27] S. Ashhab, J. R. Johansson, A. M. Zagoskin, and F. Nori, Two-level systems driven by large-amplitude fields, Phys. Rev. A **75,** 063414 (2007).

[28] K. L. Ekinci, X. M. H. Huang, and M. L. Roukes, Ultrasensitive nanoelectromechanical mass detection, Appl. Phys. Lett. **84,** 4469 (2004).

[29] J. Chaste, A. Eichler, J. Moser, G. Ceballos, R. Rurali, and A. Bachtold, A nanomechanical mass sensor with yoctogram resolution, Nat. Nanotechnol. **7,** 301 (2012).

[30] M. Li, H. X. Tang, and M. L. Roukes, Ultra-sensitive NEMS-based cantilevers for sensing, scanned probe and very high-frequency applications, Nat. Nanotechnol. **2,** 114 (2007).

[31] H. Y. Zhou, J. Choi, S. Choi, R. Landig, A. M. Douglas, J. Isoya, F. Jelezko, S. Onoda, H. Sumiya, P. Cappellaro, H. S. Knowles, H. Park, and M. D. Lukin, Quantum Metrology with Strongly Interacting Spin Systems, Phys. Rev. X **10,** 031003 (2020).